

Controllable and Fast Growth of High-Quality Atomically Thin and Atomically Flat Bi₂O₂Se Films

Yusen Feng,^{1,‡} Pei Chen,^{1,‡} Nian Li,^{1,a} Suzhe Liang,² Ke Zhang,^{1,a} Minghui Xu,¹ Yan Zhao,¹ Jie Gong,¹ Shu Zhang,¹ Huaqian Leng,¹ Yuanyuan Zhou,¹ Yong Wang,¹ and Liang Qiao^{1,a}

Affiliations:

¹) School of Physics, University of Electronic Science and Technology of China, Chengdu 610054, China

²) Technical University of Munich, TUM School of Natural Sciences, Chair for Functional Materials, James-Franck-Str. 1 85748 Garching, Germany

[‡]) These authors contributed equally.

^a) Authors to whom correspondence should be addressed: nianli@uestc.edu.cn (N. L.); phyzk@uestc.edu.cn (K. Z) and liang.qiao@uestc.edu.cn (L. Q.)

Abstract

As a novel and promising 2D material, bismuth oxyselenide (Bi₂O₂Se) has demonstrated significant potential to overcome existing technical barriers in various electronic device applications, due to its unique physical properties like high symmetry, adjustable electronic structure, ultra-high electron mobility. However, the rapid growth of Bi₂O₂Se films down to a few atomic layers with precise control remains a significant challenge. In this work, the growth of two-dimensional (2D) Bi₂O₂Se thin films by the pulsed laser deposition (PLD) method is systematically investigated. By controlling temperature, oxygen pressure, laser energy density and laser emission frequency, we successfully prepare atomically thin and flat Bi₂O₂Se (001) thin films on the (001) surface of SrTiO₃. Importantly, we provide a fundamental and unique perspective toward understanding the growth process of atomically thin and flat Bi₂O₂Se films, and the growth process can be primarily summarized into four steps: i) anisotropic non-spontaneous nucleation preferentially along the step roots; ii) monolayer Bi₂O₂Se nanosheets expanding across the surrounding area, and eventually covering the entire STO substrate step; iii) vertical growth of Bi₂O₂Se monolayer in a 2D Frank-van der Merwe (FM) epitaxial growth, and iv) with a layer-by-layer 2D FM growth mode, ultimately producing an atomically flat and epitaxially aligned thin film. Moreover, the combined results of the crystallinity quality, surface morphology and the chemical states manifest the successful PLD-growth of high-quality Bi₂O₂Se films in a controllable and fast mode.

Keywords: Bi₂O₂Se, atomically flat, atomically thin, pulsed laser deposition, epitaxial growth

Introduction

Due to the merits of moderate bandgap, excellent stability, and abundant nature retention, silicon has been a dominated semiconductor in microelectronic industry for more than 60 years.^{1,2} However, when the thickness is less than 10 nm, silicon shows a reduced carrier mobility and a serious short-channel effect, which limits the further development of the silicon-based industry. In order to solve these problems and broaden Moore's Law, novel atomically thin 2D materials linked by weak van der Waals (vdW) force substitution of strong chemical bonding connections have received a lot of attentions, such as transition metal dichalcogenides (MoS₂ and WS₂), topological insulators (Bi₂Te₃ and Bi₂Se₃), black phosphorus and monolayer elemental films (Ge, Sn, silicene, etc).³⁻⁶ Recently, a layered material, bismuth oxyselenide (Bi₂O₂Se) is regarded as one of the most promising candidates for the next-generation electronic industry due to its high electron mobility (450 cm² V⁻¹ s⁻¹, room temperature),^{7,8} moderate and tunable bandgap (~0.8 eV, up to 1.5 eV depending on thickness),^{3,7,9} and excellent ambient stability.^{7,10,11} Besides, Bi₂O₂Se can also be used in many other fields, including memristors,^{12,13} ultrafast spectroscopy,¹⁴ photocatalysis,¹⁵ terahertz switches,¹⁶ field-effect transistors,⁷ photodetector,^{17,18} solar cells,¹⁹ etc. The prerequisite for these various applications is the fabrication of Bi₂O₂Se materials. Although most study focus on the bulk crystals and multiplayer films, achievement of atomically thin Bi₂O₂Se films and atomically flat Bi₂O₂Se films deserves more efforts, with consideration of a large quantity of use in electronic industry.

Generally, Bi₂O₂Se films can be achieved via various methods, such as chemical vapor deposition (CVD),⁷ molecular beam epitaxy (MBE),²⁰ pulsed laser deposition (PLD),^{10,21} and solution-assisted methods. However, only the self-limiting vapor-solid deposition and MBE methods have been successfully applied for the atomical growth of low-dimensional Bi₂O₂Se thin films. For example, Khan et al. used the self-limiting vapor-solid method to obtain few-layer single crystal domains on a mica substrate;²² Liang et al. exploited MBE to precisely control the growth of monolayer Bi₂O₂Se on a SrTiO₃ (STO) substrate.²⁰ Compared to these two methods (CVD and MBE), PLD can combine advantages of the fast and controllable growth. However, there have been no reported on PLD-grown Bi₂O₂Se film with a monolayer or atomically flat surface of a large-scale area and a high quality. Importantly, the growth process for the Bi₂O₂Se films down to a few atomic layers has not been revealed in detail so far.

Therefore, in this work, we present a PLD approach to grow atomically thin and flat Bi₂O₂Se films with high quality in a large-scale area. We thoroughly investigate the effects of various parameters on the regulation of film growth by the PLD method. With precise optimization of the parameters, including growth temperature, laser energy density, laser emission frequency and oxygen pressure, a high-quality growth mode of 2D atomically flat Bi₂O₂Se thin films is achieved on a (001)-oriented STO substrate in a fast speed. Furthermore, the key growth processes of Bi₂O₂Se on STO are elucidated with the aid of atomic force microscopy (AFM), X-ray diffraction (XRD), and high-resolution X-ray photoelectron spectroscopy (HRXPS), which also provide the evidence of the quality of obtained atomically thin and atomically flat films. Notably, the atomically flat film structure is clearly

and directly visible in the AFM images. An intertwined weave structure is observed on the $\text{Bi}_2\text{O}_2\text{Se}$ films prepared by the PLD method, which, in conjunction with other results, demonstrates the successful fabrication of higher-quality $\text{Bi}_2\text{O}_2\text{Se}$ films using PLD in a controllable and fast mode, as compared to MBE and CVD. This knowledge is expected as an essential piece required to broaden the application of $\text{Bi}_2\text{O}_2\text{Se}$ films.

Results and Discussion

As illustrated in Figure 1a, the as-obtained target is mounted to the rotator and subjected to laser illumination with a stable emission frequency and emission intensity provided by 248 nm wavelength KrF laser. High vacuum level of 10^{-4} Pa is reached inside the entire chamber and after that oxygen is introduced, and target-substrate distance is set to 5.0 cm. Upon laser irradiation, the high-energetic species ablated from the target condense on the etched STO substrate, and then $\text{Bi}_2\text{O}_2\text{Se}/\text{STO}$ films can be obtained after cooling. By rationally adjusting the parameters of temperature, oxygen pressure, energy density and emission frequency, we can obtain a series of films. Figure 1b shows the crystal structures of $\text{Bi}_2\text{O}_2\text{Se}$ and STO. As a cubic perovskite oxide, STO (001) has a lattice parameter of $a = 3.90 \text{ \AA}$, which provides perfect lattice matching with $\text{Bi}_2\text{O}_2\text{Se}$ ($\approx 0.5\%$ mismatch) of a tetragonal structure ($I4/mmm$, $a = b = 3.887 \text{ \AA}$, $c = 12.202 \text{ \AA}$, $Z = 2$).²³ Scanning transmission electron microscopy (STEM) and First-Principle calculation provide an insight that Bi-TiO₂ is the most closely bound way of interface epitaxial growth for $\text{Bi}_2\text{O}_2\text{Se}$.^{20,24}

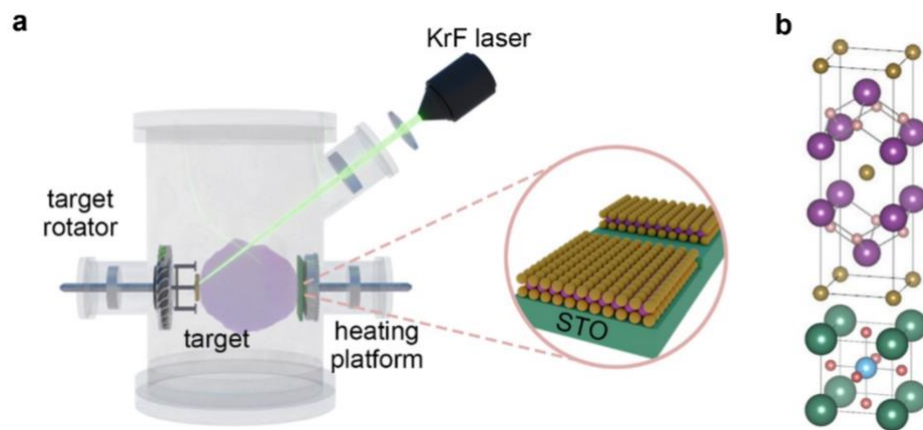


Figure 1. a) Schematic illustration of epitaxial growth of atomically flat $\text{Bi}_2\text{O}_2\text{Se}$ on the (001)-oriented STO substrate by PLD method, b) crystal structure of $\text{Bi}_2\text{O}_2\text{Se}$ and STO.

Upon reaching the substrate, the species or atoms would undergo various processes, including surface diffusion, surface migration, re-evaporation, adsorption, and condensation.²⁵ During epitaxial growth, nucleation accompanied by condensation is considered a non-spontaneous process.²⁶ From a thermodynamic perspective, by analyzing the Gibbs free energy change and the energy equilibrium condition at all interfaces, we can determine

that a lower temperature reduces the critical size required for nucleation, resulting in a lower critical free energy barrier. This, in turn, benefits for the formation of thin, continuous films with fine grains. However, if the temperature is too low, it can hinder surface diffusion, leading to condensation at low-energy chemisorption sites, which disrupts epitaxial growth and crystallization. If temperatures closer to the equilibrium temperature can produce coarser single-crystal structures. But, excessively high temperatures can exacerbate re-evaporation, and thus it is challenging to accomplish adsorption and condensation processes.²⁵ As shown in Figure 2a, the XRD patterns of Bi₂O₂Se films prepared at different temperatures indicate that single crystals can be formed at 400-510 °C, while it is difficult to condense into a film at 550 °C. We can also know from Figure 2a that the intensity of diffraction peak and its full width at half maximum (FWHM) are optimized at about 450 °C. Figure 2b shows the amplification of the (004) diffraction peaks at temperatures of 430, 450, 470, and 490 °C. The clearly visible Laue oscillations and Kiessig fringes suggest that a high and coherent out-of-plane order over the entire thickness.¹⁰ The emergence of Laue oscillations at the sample of 450 °C is generally taken as the evidence of the homogeneity of the film and smoothness of the interface, thus implying that 450 °C is an optimal growth temperature (Figure 2b). In addition, the AFM images of the films at different temperatures (Fig. S1) can support that 450 °C plays as a critical temperature for the surface roughness of the films. That is a local minimum root mean square (RMS) value at 450 °C.

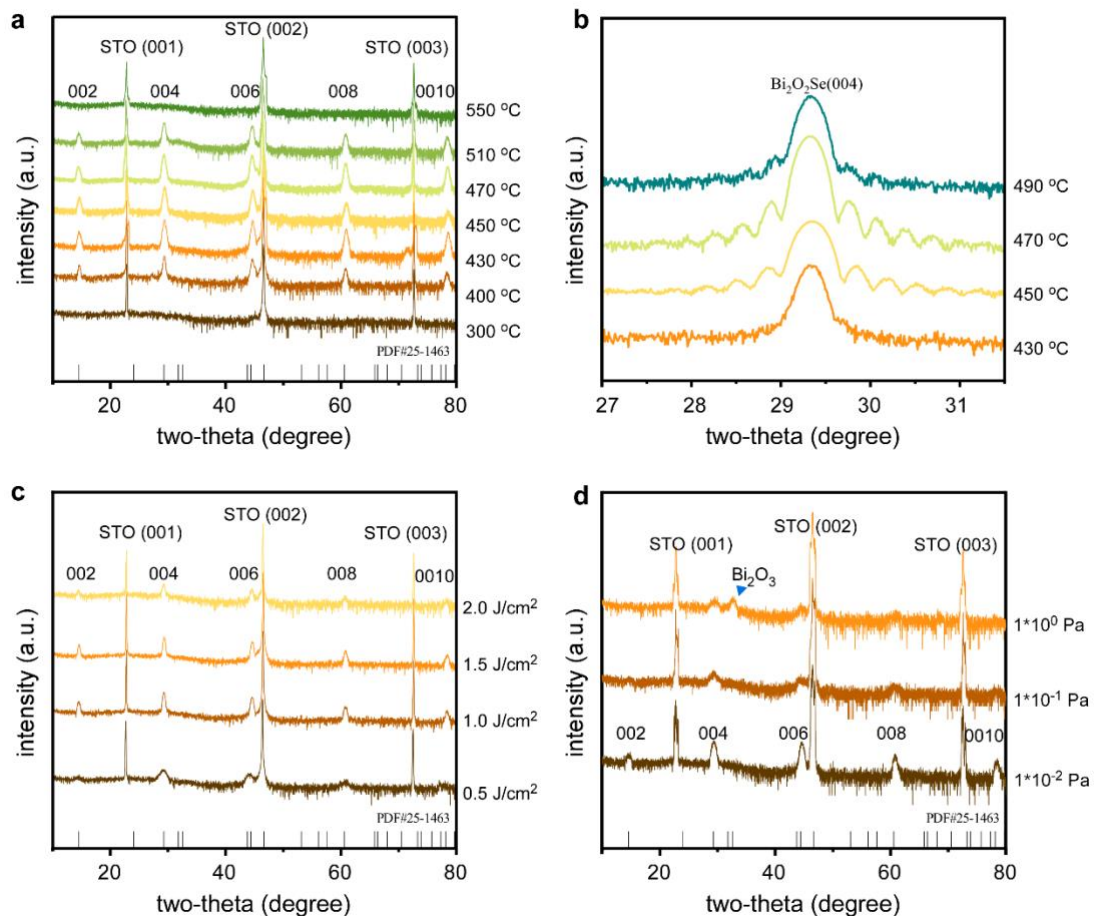


Figure 2. Effects of different conditions on the growth of thin films. a) Out-of-plane XRD patterns of Bi₂O₂Se films prepared at different temperatures. b) Bi₂O₂Se (004) XRD peak of films grown at different temperatures of 430 °C, 450 °C, 470 °C, 490 °C. Laue oscillations indicate a high and coherent out-of-plane order over the entire thickness. c) XRD patterns of Bi₂O₂Se films prepared with different laser energy densities. d) XRD patterns of Bi₂O₂Se films prepared at oxygen pressures of 1×10⁰ Pa, 1×10⁻¹ Pa, and 1×10⁻² Pa.

In contrast to temperature, the deposition rate exhibits a negative correlation with both the critical nucleus size and the change in the free energy of nucleation. Therefore, to achieve fine-grained continuous films, a higher deposition rate is required, which can be facilitated by employing lasers with high emission frequency and high energy density, as well as reducing the oxygen pressure.²⁵ Through Bi₂O₂Se (006) diffraction peaks, we obtain lattice constants and grain sizes at different emission frequencies by Bragg's Law ($2d\sin\theta = n\lambda$) and Scherrer Formula ($D = \frac{k\lambda}{\beta\cos\theta}$). Our research investigates a range of laser emission frequencies from 1 Hz to 9 Hz, and laser energy densities from 0.5 J/cm² to 2.0 J/cm². XRD data collected under all these experimental conditions (Fig. S2a and Figure 2c) consistently show the formation of single-crystal structures. Fig. S2b,c display that with emission frequency increase, the crystallite and growth rate increase as well, but the lattice constant show a fluctuation trend. Thus, the high emission frequency of 9 Hz can improve the crystallinity of the Bi₂O₂Se film, and simultaneously we can obtain a relatively low RMS roughness value (Fig. S3). Similarly, as the laser energy density increases (Fig. S4), the growth rate overall increases but the lattice constant decreases and gradually gets closer to the theoretical value (12.164 Å). However, as shown in Fig. S5, a high laser energy density adopted here is unsuitable, which shows a high RMS value. We assume that a high laser energy density will promote surface diffusion and grain coalescence (known as the Oswald annexation or fusion). This process contains the merging of smaller grains to form larger grains, thus further disrupting surface flatness and the 2D Frank-van der Merwe (FM) growth mode, and finally leading to an island growth.

Tuning the oxygen pressure to affect surface diffusion in a way that promotes the desired crystal structure and smooth film growth. Figure 2d and Fig. S6 show the XRD and AFM of the films prepared at oxygen pressures of 1 × 10⁰ Pa, 1 × 10⁻¹ Pa and 1 × 10⁻² Pa, respectively. The AFM results indicate 3D Volmer Weber (VW) growth mode at 1 × 10⁻² Pa oxygen pressures, at which Bi₂O₂Se is deposited in the form of island-like particles, and that may be related to the vacancy of oxygen atoms due to the insufficient oxygen involved in the reaction. Whereas, 2D FM growth mode is exhibited at 1 × 10⁻¹ Pa oxygen pressure (Fig. S6b,e; terrace-like structure observed), which is more favorable for us to grow high-quality atomically thin and atomically flat films. 1 × 10⁰ Pa oxygen pressure will also cause growth mode of 3D VW, due to the fact that excess oxygen leads to the formation of heterogeneous phases. Besides the surface morphologies, we continue to compare the crystal phase among these three samples. Besides the Bi₂O₂Se phase, we can also find Bi₂O₃ diffraction peaks in the 1 × 10⁰ Pa sample, which can prove that the impurity phase is formed (denoted with an arrow in Figure 2d).

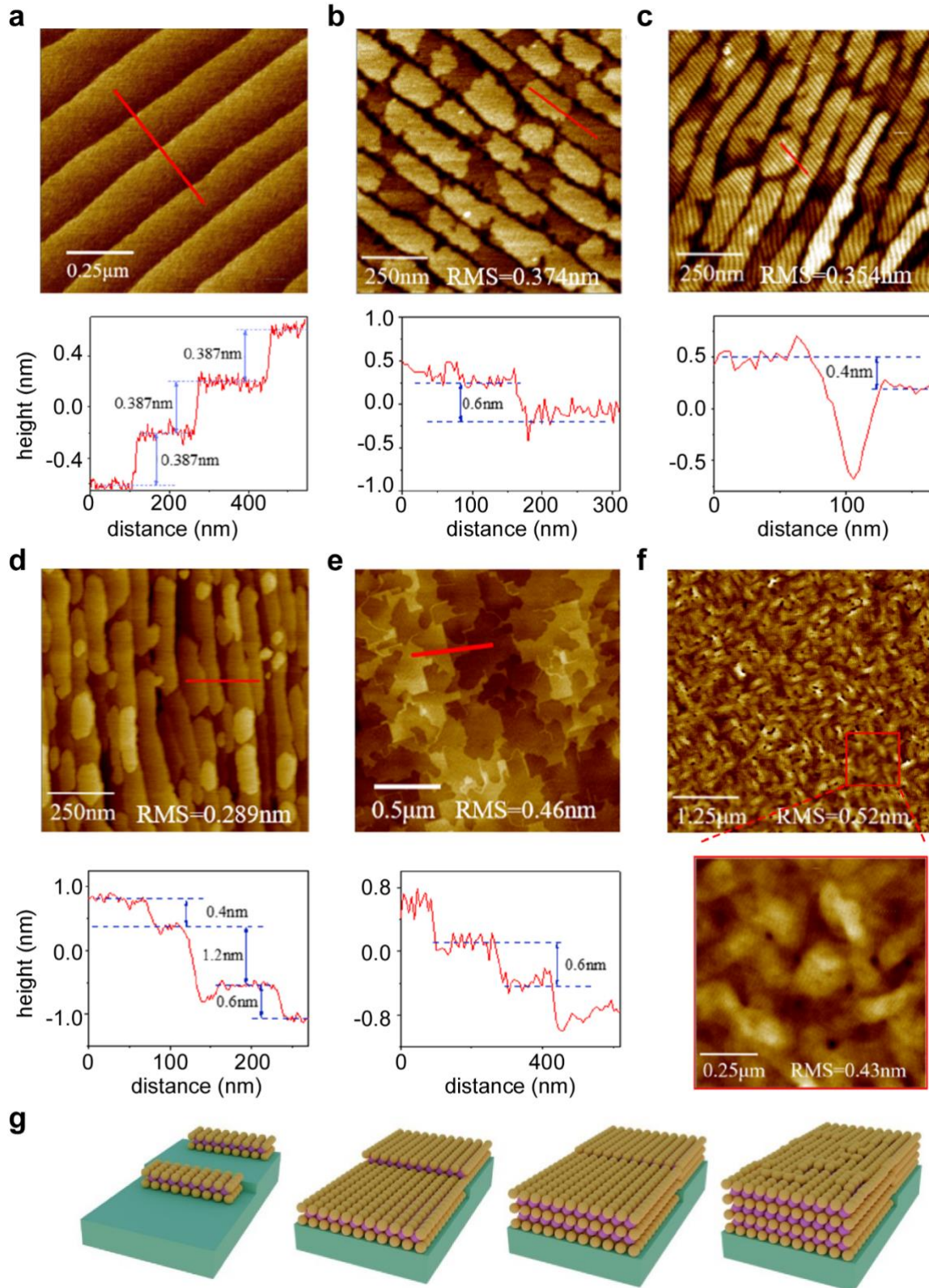


Figure 3. Growth processes of atomically flat $\text{Bi}_2\text{O}_2\text{Se}$. a) Surface morphology of TiO_2 -terminated STO substrate, showing clear terraces with a step height of 0.387 nm . b-f) Surface morphology of $\text{Bi}_2\text{O}_2\text{Se}$ films with different thicknesses: b,c) monolayer, d) 6 nm , e) 147 and f) 35 nm . g) Schematic illustration of $\text{Bi}_2\text{O}_2\text{Se}$ film grown on the (001) surface of STO .

Following a comprehensive investigation of each individual parameter, including single-crystal growth rate, grain size, flatness, and epitaxial growth quality, we have identified an optimal growth environment: a temperature of 450 °C, an oxygen pressure of 3.7×10^{-1} Pa, and a laser energy density of 0.5 J/cm² with an emission frequency of 9 Hz. This condition is employed to grow a series of Bi₂O₂Se thin films with varying thicknesses on etched STO (001) substrates with stepped TiO₂ termination. Previous studies have reported that, TiO₂-terminated STO readily coordinates with Bi₂O₂²⁺ to form a compound [BiTiO₄]¹⁻,²⁷ which facilitates the binding of Bi₂O₂Se to STO substrate. Furthermore, the creation of a 2D electron gas (2DEG) requires an STO substrate with TiO₂ termination,²⁸ which exhibits an exceptionally high carrier mobility (exceeding 10⁴ cm² V⁻¹ s⁻¹) at the perovskite heterojunction.²⁸⁻³⁰ To prepare etched substrates, we use a BHF buffer solution etching method (more details provided in Supplementary Information, Experiment section). As displayed in Figure 3a, high-quality etched substrates with a step width around 150 nm are chosen. The AFM pattern shows that the chosen substrates have an excellent flatness with a step height of 0.387 nm, which is comparable to the lattice constant of perovskite-structure STO lattice and also to the spacing of the two TiO₂ termination.

Figures 3b-d and 3g illustrate the AFM images and a schematic diagram of the growth process of Bi₂O₂Se thin films. During the initial nucleation stage, Bi₂O₂Se exhibits preferential growth along the step roots, forming monolayer Bi₂O₂Se nanosheets with a rim. This process creates a new step in the original plane, with a height of approximately 0.6 nm (Figure 3b), corresponding to the thickness of a combined [Bi₂O₂]²ⁿ⁺ and [Se]²ⁿ⁻ layer. Subsequently, the single-layer Bi₂O₂Se nanosheets will expand to the surrounding area. As they grow, adjacent nanosheets will merge and eventually cover the entire STO step. At this stage, a V-shaped trench forms, comprising the Bi₂O₂Se step, the STO step, and the Bi₂O₂Se step on the next layer. Notably, the height difference between the two Bi₂O₂Se steps is consistent with the STO layer height difference of 0.387 nm.

As the sputtered Bi₂O₂Se plasma continues to be deposited, the monolayer grows upward in a 2D FM mode. Although ions in the V-trench have the ability to form bonds on multiple sides, the 0.389 nm height difference between adjacent SrTiO₃ steps causes the upper and lower Bi₂O₂Se layers to become misaligned. Furthermore, the identical height of the upper [Bi₂O₂]²ⁿ⁺ layer and lower [Se]²ⁿ⁻ layer would result in a significant increase in interfacial energy if newly adsorbed atoms were to condense into the V-shaped trench, thereby increasing the total energy of the system. As a result, the V-shaped trench is retained. As shown in Figure 3c, lattice mismatch leads to gaps in the same layer of Bi₂O₂Se, and then the film will continue to generate multiple layers upwards. Figure 3d shows that the preferential growth of some regions creates a larger step height difference, which would make it possible to grow along the step gradient. If the transverse growth exceeds the width of the next step, it can connect to the step further down, forming a transverse sheet. Ultimately, the diffusion and connection of the sheets along the step with the transverse sheet give rise to a crossed textile structure. The AFM pattern of textile structure can be seen in Figure 3f. According to previous studies,³¹ Se vacancies can also form textile structures, but it is

not clear whether there is any correlation between the two textile structures. It can be seen that 147 nm-thick $\text{Bi}_2\text{O}_2\text{Se}$ films do not show strip-like steps, but exhibits a regional lamellar structure (Figure 3e). The height of adjacent steps is still consistent with the height of single $\text{Bi}_2\text{O}_2\text{Se}$ layer, which suggests the film well maintains a 2D FM layer-by-layer growth mode and that the mismatches between the regions have been resolved. X-ray reflectivity (XRR) measurements (Fig. S7) reveal the presence of oscillations in the reflectivity curve for the 147 nm thick film, which signifies a coherent out-of-plane structural order throughout the entire thickness of the film. All these samples show a single crystal phase without impurities (Fig. S8).

To have an in-depth understanding about the crystallinity of the $\text{Bi}_2\text{O}_2\text{Se}$ samples, the rocking curves of the $\text{Bi}_2\text{O}_2\text{Se}$ (004) peaks are examined. The ω -rocking curve of the $\text{Bi}_2\text{O}_2\text{Se}$ (004) peak, as shown in Figure 4a, is relatively narrow, and has a FWHM of $\sim 0.07^\circ$, consistent with the fact that $\text{Bi}_2\text{O}_2\text{Se}$ deposited on STO has a low lattice mismatch and grow structurally similar directions. We further examined the in-plane crystal structure of $\text{Bi}_2\text{O}_2\text{Se}$ epitaxial thin films deposited at 450°C . As shown in azimuth Φ scans of the off-axis $\{011\}$ peaks of STO substrate and the $\text{Bi}_2\text{O}_2\text{Se}$ film (Figure 4b), the four peaks separated by 90° are present in these two films, which confirms the in-plane alignment of the $\text{Bi}_2\text{O}_2\text{Se}$ film with the STO substrate.^{10,20} The $\text{Bi}_2\text{O}_2\text{Se}$ and STO peaks are located at the same angular position, indicating that the unit cells show no rotation with respect to one another. Thus, we can conclude that the $\text{Bi}_2\text{O}_2\text{Se}$ films deposited on STO via PLD method show a high crystal quality. Figure 4c shows the growth rate of $\text{Bi}_2\text{O}_2\text{Se}$ film grown on STO is about 5.9 nm/min, which is about 11 times faster than that of multilayer $\text{Bi}_2\text{O}_2\text{Se}/\text{STO}$ films realized by the CVD method and about 196 times faster than the MBE method.^{20,21} Higher growth rates mean lower production costs, which suggests that synthesis of high-quality $\text{Bi}_2\text{O}_2\text{Se}$ films by PLD method holds excellent promise for industrial applications.

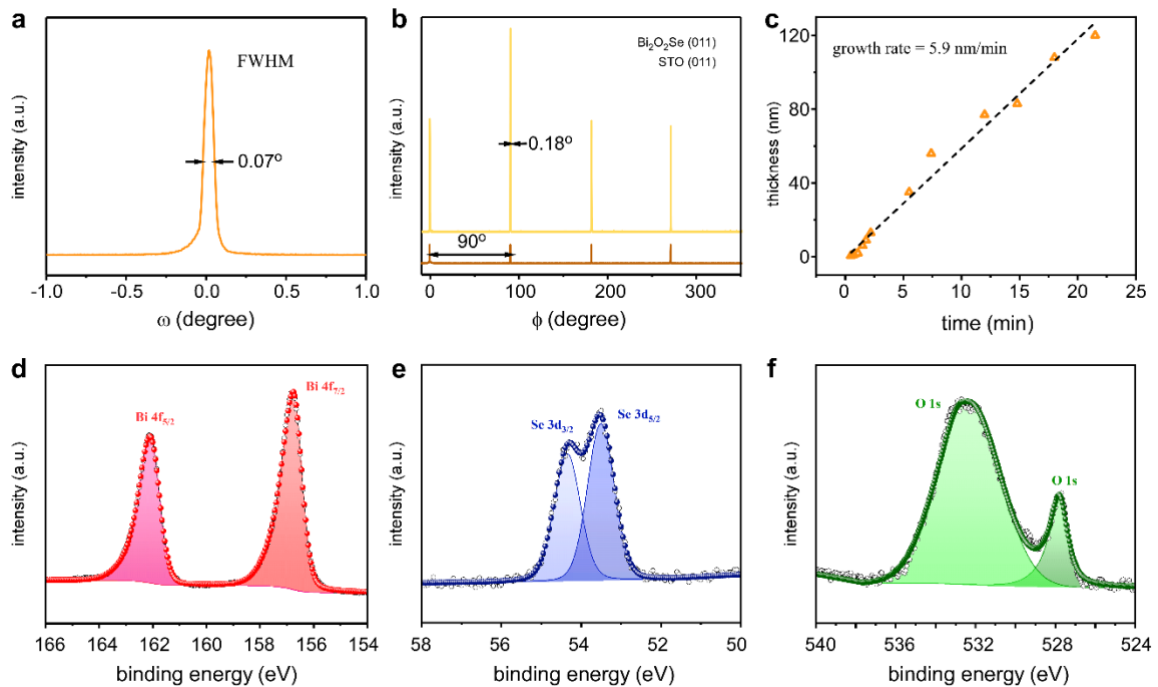


Figure 4. Quality inspection of the films grown at 450 °C. a) The ω -rocking curve of corresponding (004) reflection. b) Azimuth Φ scans of the off-axis {011} peaks of STO substrate and the Bi₂O₂Se film. c) Plot of film thickness versus deposition time, showing a growth rate of 5.9 nm/min. d-f) X-ray photoemission spectra of 35 nm-thick Bi₂O₂Se/STO film.

The electronic properties of 35 nm Bi₂O₂Se film are characterized using HRXPS. As shown in Figure 4d, the two spin-orbital-coupling (SOC) symmetric peaks of Bi 4f_{7/2} and Bi 4f_{5/2} are centered at 156.8 eV and 162.1 eV, which can be attributed to the Bi peak in the O-Bi bond.^{3,32,33} Similarly, according to the effect of SOC, the Se 3d peak is split into two Lorentz peaks centered at 53.5 eV and 54.4 eV (Figure 4e), corresponding to the Se 3d_{5/2} and Se 3d_{3/2}.^{3,32} The fitted results of the peaks are all within a reasonable chemical shift range,^{34,35} which is also confirmed by the HRXPS data of the Bi₂O₂Se film at different specific thicknesses (Fig. S9). Thus, we reason that the Bi₂O₂Se film have a high quality in its chemical state.

Conclusion

In conclusion, we have systematically explored the impact of various fabrication parameters, involving growth temperature, laser energy density, laser emission frequency and oxygen pressure, on the film properties by PLD method and using etched STO (001) substrates, and simultaneously have gained a deep understanding of the growth mechanism for Bi₂O₂Se films. The growth process can be primarily summarized into four steps: 1) anisotropic non-spontaneous nucleation preferentially along the step roots; 2) monolayer Bi₂O₂Se nanosheets expanding across the surrounding area, and eventually cover the entire STO substrate step; 3) monolayer Bi₂O₂Se grows vertically in a 2D FM epitaxial growth, and 4) with a layer-by-layer 2D FM growth mode, ultimately producing an atomically flat and epitaxially aligned thin film. By precisely controlling the thickness of Bi₂O₂Se films grown via a 2D FM mode, we successfully prepared atomically thin and atomically flat Bi₂O₂Se films on STO substrate with TiO₂ termination, exhibiting epitaxial quality superior to that of previously reported Bi₂O₂Se/STO films grown by PLD methods. Notably, the film growth rate in the present study reaches 5.9 nm/min, offering a significant cost advantage over other methods, like MBE, for large-scale industrial fabrication. Furthermore, XRD and HRXPS measurements verify that the Bi₂O₂Se films exhibit excellent epitaxial growth with high crystallinity quality and chemical homogeneity.

Supplementary Material

See supplementary material for the experimental details, the surface morphology of Bi₂O₂Se films at different temperatures, XRD data of Bi₂O₂Se films at different emission frequencies, XRD data of Bi₂O₂Se films at different laser energy densities, surface morphology of Bi₂O₂Se films at different laser energy densities, surface morphology of Bi₂O₂Se films at different oxygen pressures, X-ray reflected pattern of different thicknesses and XPS data of Bi₂O₂Se films at representative thicknesses.

Acknowledgements

This work was supported by funding from the National Science Foundation of China (12304078, 52072059), Natural Science Foundation of Sichuan Province (2024NSFSC1384).

AUTHOR DECLARATIONS

Conflict of Interest

The authors have no conflicts to disclose.

Author Contributions

Yusen Feng and Pei Chen equally contributed to this work.

Yusen Feng: Data curation (supporting); Formal analysis (equal); Investigation (equal); Methodology (equal); Writing -original draft (main); Writing – review & editing (equal). **Pei Chen:** Data curation (main); Formal analysis (equal); Investigation (equal); Methodology (equal). **Nian Li:** Conceptualization (equal); Data curation (supporting); Investigation (equal); Methodology (equal); Project administration (equal); Supervision (equal); Writing -original draft (supporting); Writing – review & editing (equal). **Suzhe Liang:** Data curation (supporting); Visualization (equal); Writing – review & editing (equal). **Ke Zhang:** Conceptualization (supporting); Investigation (equal); Methodology (equal); Project administration (equal); Supervision (equal); Writing -original draft (supporting); Writing – review & editing (equal). **Yan Zhao:** Investigation (equal); Writing – review & editing (supporting). **Minghui Xu:** Investigation (equal); Writing – review & editing (supporting). **Jie Gong:** Investigation (equal); Writing – review & editing (supporting). **Shu Zhang:** Investigation (equal); Writing – review & editing (supporting). **Huaqian Leng:** Formal analysis (equal); Writing – review & editing (supporting). **Yuanyuan Zhou:** Formal analysis (equal); Writing – review & editing (supporting). **Yong Wang:** Formal analysis (equal); Writing – review & editing (supporting). **Liang Qiao:** Conceptualization (equal); Data curation (supporting); Formal analysis (equal); Funding acquisition (main); Investigation (equal); Methodology (equal); Project administration (equal); Resources (main); Supervision (equal); Validation (equal); Writing -original draft (supporting); Writing – review & editing (equal).

DATA AVAILABILITY

The data that support the findings of this study are available from the corresponding author upon reasonable request.

References

- ¹ J.S. Kilby, "Invention of the integrated circuit," *IEEE Trans. Electron Devices* **23**(7), 648–654 (1976).
- ² A.I. Kingon, J.-P. Maria, and S.K. Streiffer, "Alternative dielectrics to silicon dioxide for memory and logic devices," *Nature* **406**(6799), 1032–1038 (2000).
- ³ J. Wu, C. Tan, Z. Tan, Y. Liu, J. Yin, W. Dang, M. Wang, and H. Peng, "Controlled Synthesis of High-Mobility Atomically Thin Bismuth Oxyselenide Crystals," *Nano Lett.* **17**(5), 3021–3026 (2017).
- ⁴ T. Tong, M. Zhang, Y. Chen, Y. Li, L. Chen, J. Zhang, F. Song, X. Wang, W. Zou, Y. Xu, and R. Zhang, "Ultra-high Hall mobility and suppressed backward scattering in layered semiconductor Bi₂O₂Se," *Appl. Phys. Lett.* **113**(7), 072106 (2018).
- ⁵ X. Ding, Y. Zhao, H. Xiao, and L. Qiao, "Engineering Schottky-to-Ohmic contact transition for 2D metal–semiconductor junctions," *Appl. Phys. Lett.* **118**(9), 091601 (2021).
- ⁶ X. Ding, S. Zhang, M. Zhao, Y. Xiang, K.H.L. Zhang, X. Zu, S. Li, and L. Qiao, "NbS₂: A Promising *p*-Type Ohmic Contact for Two-Dimensional Materials," *Phys. Rev. Appl.* **12**(6), 064061 (2019).
- ⁷ J. Wu, H. Yuan, M. Meng, C. Chen, Y. Sun, Z. Chen, W. Dang, C. Tan, Y. Liu, J. Yin, Y. Zhou, S. Huang, H.Q. Xu, Y. Cui, H.Y. Hwang, Z. Liu, Y. Chen, B. Yan, and H. Peng, "High electron mobility and quantum oscillations in non-encapsulated ultrathin semiconducting Bi₂O₂Se," *Nat. Nanotechnol.* **12**(6), 530–534 (2017).
- ⁸ Z. Zhu, X. Yao, S. Zhao, X. Lin, and W. Li, "Giant Modulation of the Electron Mobility in Semiconductor Bi₂O₂Se via Incipient Ferroelectric Phase Transition," *J. Am. Chem. Soc.* **144**(10), 4541–4549 (2022).
- ⁹ Yu.M. Koroteev, G. Bihlmayer, J.E. Gayone, E.V. Chulkov, S. Blügel, P.M. Echenique, and Ph. Hofmann, "Strong Spin-Orbit Splitting on Bi Surfaces," *Phys. Rev. Lett.* **93**(4), 046403 (2004).
- ¹⁰ Y. Song, Z. Li, H. Li, S. Tang, G. Mu, L. Xu, W. Peng, D. Shen, Y. Chen, X. Xie, and M. Jiang, "Epitaxial growth and characterization of high quality Bi₂O₂Se thin films on SrTiO₃ substrates by pulsed laser deposition," *Nanotechnology* **31**(16), 165704 (2020).
- ¹¹ U. Khan, A. Nairan, K. Khan, S. Li, B. Liu, and J. Gao, "Salt-Assisted Low-Temperature Growth of 2D Bi₂O₂Se with Controlled Thickness for Electronics," *Small* **19**(10), 2206648 (2023).
- ¹² Z. Dong, Q. Hua, J. Xi, Y. Shi, T. Huang, X. Dai, J. Niu, B. Wang, Z.L. Wang, and W. Hu, "Ultrafast and Low-Power 2D Bi₂O₂Se Memristors for Neuromorphic Computing Applications," *Nano Lett.* **23**(9), 3842–3850 (2023).
- ¹³ Z. Zhang, T. Li, Y. Wu, Y. Jia, C. Tan, X. Xu, G. Wang, J. Lv, W. Zhang, Y. He, J. Pei, C. Ma, G. Li, H. Xu, L. Shi, H. Peng, and H. Li, "Truly Concomitant and Independently Expressed Short- and Long-Term Plasticity in a Bi₂O₂Se-Based Three-Terminal Memristor," *Adv. Mater.* **31**(3), 1805769 (2019).
- ¹⁴ X. Tian, H. Luo, R. Wei, C. Zhu, Q. Guo, D. Yang, F. Wang, J. Li, and J. Qiu, "An Ultrabroadband Mid-Infrared Pulsed Optical Switch Employing Solution-Processed Bismuth Oxyselenide," *Adv. Mater.* **30**(31), 1801021 (2018).
- ¹⁵ D. Ding, Z. Jiang, D. Ji, M. Nosang Vincent, and L. Zan, "Bi₂O₂Se as a novel co-catalyst for photocatalytic hydrogen evolution reaction," *Chem. Eng. J.* **400**, 125931 (2020).
- ¹⁶ Z.W. Li, and J.-S. Li, "Bi₂O₂Se for broadband terahertz wave switching," *Appl. Opt.* **59**(35), 11076 (2020).
- ¹⁷ Y. Chen, W. Ma, C. Tan, M. Luo, W. Zhou, N. Yao, H. Wang, L. Zhang, T. Xu, T. Tong, Y. Zhou, Y. Xu, C. Yu, C. Shan, H. Peng, F. Yue, P. Wang, Z. Huang, and W. Hu, "Broadband Bi₂O₂Se Photodetectors from Infrared to Terahertz," *Adv. Funct. Mater.* **31**(14), 2009554 (2021).
- ¹⁸ J. Li, Z. Wang, J. Chu, Z. Cheng, P. He, J. Wang, L. Yin, R. Cheng, N. Li, Y. Wen, and J. He, "Oriented layered Bi₂O₂Se nanowire arrays for ultrasensitive photodetectors," *Appl. Phys. Lett.* **114**(15), 151104 (2019).
- ¹⁹ C. Huang, and H. Yu, "Two-Dimensional Bi₂O₂Se with High Mobility for High-Performance Polymer Solar Cells," *ACS Appl. Mater. Interfaces* **12**(17), 19643–19654 (2020).

- ²⁰ Y. Liang, Y. Chen, Y. Sun, S. Xu, J. Wu, C. Tan, X. Xu, H. Yuan, L. Yang, Y. Chen, P. Gao, J. Guo, and H. Peng, “Molecular Beam Epitaxy and Electronic Structure of Atomically Thin Oxyselenide Films,” *Adv. Mater.* **31**(39), 1901964 (2019).
- ²¹ C. Tan, M. Tang, J. Wu, Y. Liu, T. Li, Y. Liang, B. Deng, Z. Tan, T. Tu, Y. Zhang, C. Liu, J.-H. Chen, Y. Wang, and H. Peng, “Wafer-Scale Growth of Single-Crystal 2D Semiconductor on Perovskite Oxides for High-Performance Transistors,” *Nano Lett.* **19**(3), 2148–2153 (2019).
- ²² U. Khan, L. Tang, B. Ding, L. Yuting, S. Feng, W. Chen, M.J. Khan, B. Liu, and H. Cheng, “Catalyst-Free Growth of Atomically Thin Bi₂O₂Se Nanoribbons for High-Performance Electronics and Optoelectronics,” *Adv. Funct. Mater.* **31**(31), 2101170 (2021).
- ²³ C. Drasar, P. Ruleova, L. Benes, and P. Lostak, “Preparation and Transport Properties of Bi₂O₂Se Single Crystals,” *J. Electron. Mater.* **41**(9), 2317–2321 (2012).
- ²⁴ X.-L. Zhu, P.-F. Liu, G. Xie, and B.-T. Wang, “First-principles study of thermal transport properties in the two- and three-dimensional forms of Bi₂O₂Se,” *Phys. Chem. Chem. Phys.* **21**(21), 10931–10938 (2019).
- ²⁵ T. Minbo, and L. Zheng, editors, *Bo mo ji shu yu bo mo cai liao*, Di 1 ban (Qing hua da xue chu ban she, Beijing, 2011).
- ²⁶ H. Gu, J. Zhang, J. Sun, G. Wu, and Z. Sun, “Refinement behaviour of microstructure in in-situ synthesised (TiB+TiC)/Ti₆Al₄V composites by laser melting deposition,” *Mater. Sci. Technol.* **39**(17), 2662–2669 (2023).
- ²⁷ M. Kang, H.B. Jeong, Y. Shim, H.-J. Chai, Y.-S. Kim, M. Choi, A. Ham, C. Park, M. Jo, T.S. Kim, H. Park, J. Lee, G. Noh, J.Y. Kwak, T. Eom, C.-W. Lee, S.-Y. Choi, J.M. Yuk, S. Song, H.Y. Jeong, and K. Kang, “Layer-Controlled Growth of Single-Crystalline 2D Bi₂O₂Se Film Driven by Interfacial Reconstruction,” *ACS Nano* **18**(1), 819–828 (2024).
- ²⁸ Y. Guo, Y. Song, M. Yang, Z. Xu, H. Xie, H. Li, Z. Li, H. Liang, S. Ruan, and Y.-J. Zeng, “Unveiling interface interaction assisted broadband photoresponse of epitaxial 2D Bi₂O₂Se on perovskite oxides,” *J. Mater. Chem. C* **8**(38), 13226–13234 (2020).
- ²⁹ S. Thiel, G. Hammerl, A. Schmehl, C.W. Schneider, and J. Mannhart, “Tunable Quasi-Two-Dimensional Electron Gases in Oxide Heterostructures,” *Science* **313**(5795), 1942–1945 (2006).
- ³⁰ Y.Z. Chen, N. Bovet, F. Trier, D.V. Christensen, F.M. Qu, N.H. Andersen, T. Kasama, W. Zhang, R. Giraud, J. Dufouleur, T.S. Jespersen, J.R. Sun, A. Smith, J. Nygård, L. Lu, B. Büchner, B.G. Shen, S. Linderoth, and N. Pryds, “A high-mobility two-dimensional electron gas at the spinel/perovskite interface of γ -Al₂O₃/SrTiO₃,” *Nat. Commun.* **4**(1), 1371 (2013).
- ³¹ C. Chen, M. Wang, J. Wu, H. Fu, H. Yang, Z. Tian, T. Tu, H. Peng, Y. Sun, X. Xu, J. Jiang, N.B.M. Schröter, Y. Li, D. Pei, S. Liu, S.A. Ekahana, H. Yuan, J. Xue, G. Li, J. Jia, Z. Liu, B. Yan, H. Peng, and Y. Chen, “Electronic structures and unusually robust bandgap in an ultrahigh-mobility layered oxide semiconductor, Bi₂O₂Se,” *Sci. Adv.* **4**(9), eaat8355 (2018).
- ³² U. Khan, Y. Luo, L. Tang, C. Teng, J. Liu, B. Liu, and H. Cheng, “Controlled Vapor–Solid Deposition of Millimeter-Size Single Crystal 2D Bi₂O₂Se for High-Performance Phototransistors,” *Adv. Funct. Mater.* **29**(14), 1807979 (2019).
- ³³ D. Kong, J.J. Cha, K. Lai, H. Peng, J.G. Analytis, S. Meister, Y. Chen, H.-J. Zhang, I.R. Fisher, Z.-X. Shen, and Y. Cui, “Rapid Surface Oxidation as a Source of Surface Degradation Factor for Bi₂Se₃,” *ACS Nano* **5**(6), 4698–4703 (2011).
- ³⁴ X. Liu, D. Legut, R. Zhang, T. Wang, Y. Fan, and Q. Zhang, “Tunable magnetic order in transition metal doped, layered, and anisotropic Bi₂O₂Se: Competition between exchange interaction mechanisms,” *Phys. Rev. B* **100**(5), 054438 (2019).

³⁵ Q. Fu, C. Zhu, X. Zhao, X. Wang, A. Chaturvedi, C. Zhu, X. Wang, Q. Zeng, J. Zhou, F. Liu, B.K. Tay, H. Zhang, S.J. Pennycook, and Z. Liu, "Ultrasensitive 2D Bi₂O₂Se Phototransistors on Silicon Substrates," *Adv. Mater.* **31**(1), 1804945 (2019).